

Self-Supervised Stereo Matching with Multi-Baseline Contrastive Learning

Peng Xu, Zhiyu Xiang*, Jingyun Fu, Tianyu Pu, Kai Wang,
Chaojie Ji, Tingming Bai, Eryun Liu

College of Information Science and Electronic Engineering, Zhejiang University, China
xxxupeng@zju.edu.cn

Abstract

Current self-supervised stereo matching relies on the photometric consistency assumption, which breaks down in occluded regions due to ill-posed correspondences. To address this issue, we propose **BaCon-Stereo**, a simple yet effective contrastive learning framework for self-supervised stereo network training in both non-occluded and occluded regions. We adopt a teacher-student paradigm with multi-baseline inputs, in which the stereo pairs fed into the teacher and student share the same reference view but differ in target views. Geometrically, regions occluded in the student’s target view are often visible in the teacher’s, making it easier for the teacher to predict in these regions. The teacher’s prediction is rescaled to match the student’s baseline and then used to supervise the student. We also introduce an occlusion-aware attention map to better guide the student in learning occlusion completion. To support training, we synthesize a multi-baseline dataset **BaCon-20k**. Extensive experiments demonstrate that BaCon-Stereo improves prediction in both occluded and non-occluded regions, achieves strong generalization and robustness, and outperforms state-of-the-art self-supervised methods on both KITTI 2015 and 2012 benchmarks. Our code and dataset will be released upon paper acceptance.

Introduction

As one of the classic topics (Bai et al. 2025; Xu et al. 2025b; Zhong et al. 2025) in computer vision, stereo matching aims to recover 3D geometry by estimating the horizontal displacement (*i.e.*, disparity) between corresponding pixels in the reference and target images. It plays a crucial role in fields such as autonomous driving, augmented reality, and robotics. In recent years, fully-supervised stereo matching has achieved remarkable progress. However, training stereo networks on real-world data remains challenging, as it typically requires costly LiDAR-based disparity annotations.

Against this background, self-supervised stereo matching becomes an attractive solution, especially for fine-tuning in specific real-world scenarios. Self-supervised methods usually rely on photometric consistency as the supervision signal (Zhong, Dai, and Li 2017). However, non-overlapping fields of view between the reference and target images, along with foreground occlusions, often result in certain reference pixels being absent in the target image. These pixels violate

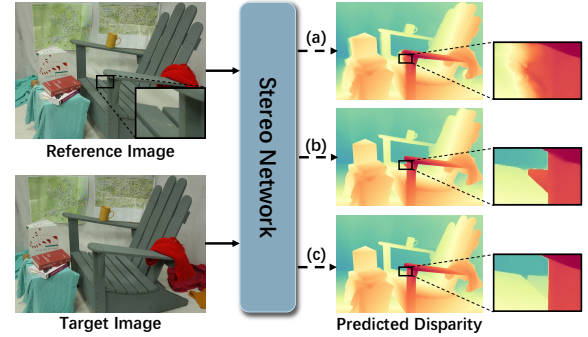


Figure 1: **An illustration of disparity prediction in occluded regions.** (a) stereo network trained by photometric loss without occlusion mask takes a “shortcut” by filling occluded regions with disparities from adjacent non-occluded areas. (b) stereo network trained by masked photometric loss makes incorrect prediction in occluded regions. (c) stereo network trained by our occlusion-aware contrastive loss achieves accurate matching and completion in non-occluded and occluded regions, respectively.

the photometric consistency assumption, leading networks to naively copy neighboring disparities to minimize photometric loss in occluded regions, as shown in Fig. 1(a).

Several recent works attempt to detect occluded pixels and exclude them from the photometric loss, thereby preventing the network from being misled during training. For example, OASM (Li and Yuan 2018) employs a sub-network to predict the occlusion mask from the reference image directly. PASMnet (Wang et al. 2022) applies a threshold on its intermediate attention map to remove pixels with low feature similarity across all candidate disparities. Although these methods improve matching performance, Fig. 1(b) shows that training exclusively in non-occluded regions is insufficient for producing reliable disparity prediction in occluded regions. We argue that accurate supervision in occluded regions is crucial for enabling stereo networks to learn effective disparity completion behavior.

In this work, we leverage additional target cues to obtain reliable pseudo-ground truth in occluded regions. Specifically, we instantiate a teacher network by duplicating the trained student network. Both the teacher and the student

*Corresponding author.

share the same reference image but are fed with different target images. Due to variations in target views and baseline lengths, their occluded regions and disparity scales differ. Nevertheless, they still need to predict consistent reference geometry. We rescale the teacher’s output disparity to match the student’s baseline and use it as pseudo-ground truth to supervise the student. We also mask out pixels that are occluded for the teacher, where the pseudo-ground truth exhibits high uncertainty. The supervision signal covers the shared non-occluded regions and areas that are teacher-friendly but student-challenging. Through this multi-baseline configuration, we supervise the student training in both occluded and non-occluded regions.

Furthermore, we observe that applying a uniform penalty across the entire image fails to adequately supervise stereo networks in occluded regions. Neural networks tend to learn simple and clear patterns first (Arpit et al. 2017), meaning that stereo networks favor learning easy matching over challenging completion. We mitigate this problem through occlusion-aware supervision that increases loss in regions occluded to the student but visible to the teacher, driving the student to actively develop occlusion completion capabilities. Finally, the student is updated via back-propagation, while the teacher’s parameters are updated using an exponential moving average of the student’s parameters.

We synthesize a multi-baseline stereo dataset BaCon-20k from CARLA simulator (Dosovitskiy et al. 2017) for training, and generate novel views from real-world binocular images for fine-tuning. Extensive ablations validate the effectiveness of our method. Moreover, our method achieves impressive zero-shot generalization and fine-tuning performance. Our main contributions are as follows:

- We propose a novel multi-baseline contrastive learning framework with a momentum teacher, enabling self-supervised stereo network training in both occluded and non-occluded regions based on geometry consistency.
- We design an occlusion-aware attention map to guide the stereo network to learn powerful completion capabilities in occluded regions.
- We synthesize a multi-baseline stereo dataset covering diverse lighting and weather conditions to support multi-baseline contrastive learning.
- Our method achieves new state-of-the-art performance among self-supervised stereo methods on both the KITTI 2015 and 2012 benchmarks.
- Our method significantly improves the zero-shot generalization of existing stereo networks and enhances the robustness under diverse weather conditions.

Related Work

Deep Stereo Matching. Over the past decades, stereo matching has undergone rapid evolution, transitioning from hand-crafted algorithms (Scharstein and Szeliski 2002) to semi-learning methods (Žbontar and LeCun 2016), and finally to end-to-end learning methods (Mayer et al. 2016). Current deep stereo methods are primarily categorized as: 3D convolution-based cost aggregation (Chang and

Chen 2018; Chen et al. 2022; Xu et al. 2025a) and ConvGRU-based iterative optimization (Lipson, Teed, and Deng 2021; Li et al. 2022). IGEVStereo (Xu et al. 2023) employs a lightweight 3D convolutional network to provide high-quality initial disparity for iterative units. Selective-Stereo (Wang et al. 2024) aggregates hidden information across multiple frequencies to improve accuracy in edge and smooth regions. DEFOM-Stereo (Jiang et al. 2025) leverages strong representations from the monocular depth foundation model (Yang et al. 2024b) to achieve impressive performance.

Self-Supervised Stereo. Self-supervised stereo matching has emerged as a promising paradigm to overcome the reliance on expensive disparity annotations. SsSnet (Zhong, Dai, and Li 2017) lays the groundwork by combining photometric consistency with disparity smoothness to train on unlabeled stereo pairs. Building on this, OASM (Li and Yuan 2018) introduces an occlusion inference module to filter out areas that do not meet the photometric consistency assumption. PVStereo (Wang et al. 2021) leverages a pyramid voting scheme to aggregate multi-scale disparity hypotheses, generating reliable pseudo-ground truth for training. PASMnet (Wang et al. 2022) applies a threshold to its intermediate attention maps, filtering out low-confidence matches that typically arise in occluded areas. UHP (Yang et al. 2024c) mitigates the incorrect guidance problem of photometric loss with 3D planar cues.

Contrastive Learning. Contrastive learning aims to learn representations by pulling positive samples closer while pushing negative samples apart in the embedding space. InstDisc (Wu et al. 2018) pioneers this direction by introducing an external memory bank to store and sample negative examples. MoCo (He et al. 2020) replaces the memory bank with a dynamic queue and introduces a momentum encoder updated via exponential moving averages, which for the first time surpasses fully-supervised counterparts on downstream tasks. BYOL (Grill et al. 2020) proposes a novel negative-sample-free paradigm and employs asymmetric networks to prevent model collapse. DINO (Caron et al. 2021) replaces convolutional backbones with vision transformer and applies centering normalization to the teacher to enhance training stability.

DualNet (Wang et al. 2025) introduces negative-free contrastive learning into stereo matching by training the teacher via feature-metric consistency in the first stage, and then using it to supervise the student’s probability distribution in the second. However, the teacher in DualNet still fails to provide accurate supervision in occluded regions. In contrast, our method feeds different target views into the student and the momentum teacher while enforcing pixel-wise geometry consistency, enabling effective supervision of the student’s occlusions within a single training stage.

Method

Preliminary

Given a pair of rectified stereo images, stereo matching aims to find the corresponding pixel in the target image I_{tgt} for each pixel in the reference image I_{ref} . The horizontal dis-

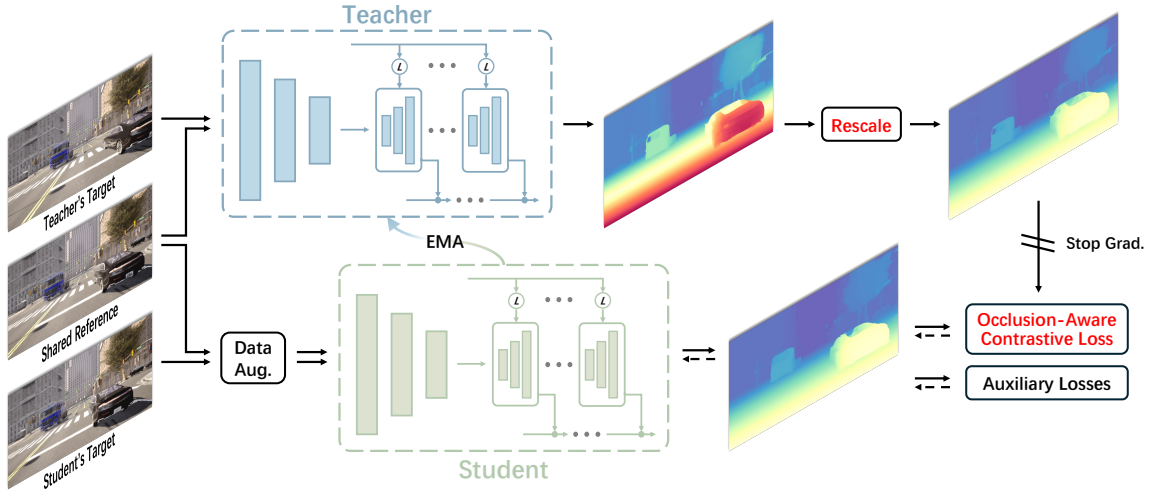


Figure 2: **Overview of our BaCon-Stereo.** Stereo pairs sharing the same reference image but different target images are fed into the teacher and student respectively. The teacher’s prediction is then rescaled to align with the student’s baseline. This multi-view configuration enables the teacher to generate reliable pseudo-ground truth for both occluded and non-occluded regions of the student. Data augmentation is used to force the student to develop robust feature representations. We apply stop-gradient operation to the teacher and update its parameters using exponential moving average (EMA) of the student’s parameters.

placement between corresponding pixels is called disparity d . Through triangulation, the depth z of each pixel in the reference image can be calculated as:

$$z = \frac{B \cdot f}{d} \quad (1)$$

where B is the baseline length, *i.e.* the distance between the two camera optical centers, and f is the focal length.

Photometric consistency assumption is usually exploited for self-supervised stereo network training (Zhong, Dai, and Li 2017). The target image I_{tgt} is reconstructed as the reference image \hat{I}_{ref} via the disparity-based warping. The photometric difference between I_{ref} and \hat{I}_{ref} is then computed as a weighted sum of the SSIM term (Wang et al. 2004) and the L_1 -norm term:

$$\mathcal{L}_p = \frac{\alpha}{2}(1 - \text{SSIM}(I_{ref}, \hat{I}_{ref})) + (1 - \alpha)\|I_{ref} - \hat{I}_{ref}\|_1 \quad (2)$$

Edge-aware smoothness loss (Zhong, Dai, and Li 2017) assists in encouraging smooth disparities in non-edge regions while preserving sharp transitions at edges:

$$\mathcal{L}_s = |\partial_x d|e^{-|\partial_x I_{ref}|} + |\partial_y d|e^{-|\partial_y I_{ref}|} \quad (3)$$

However, the photometric consistency assumption has an inherent limitation: it relies on the premise that corresponding pixels across views share similar appearance. This premise often breaks down in occluded regions, where no valid correspondence exists, misleading the supervision signal. Moreover, the smoothness loss alone is insufficient to provide adequate supervision in these challenging regions. To address this limitation, we leverage geometry consistency between stereo pairs captured with different baselines, providing effective supervision even in regions where photometric cues fail.

Multi-Baseline Contrastive Learning Framework

In this section, we introduce our multi-baseline contrastive learning framework. For clarity, we use the superscript s and t to denote the student and teacher networks respectively in the following description.

As illustrated in Fig. 2, we feed triplet-view images into the teacher and student networks to predict disparity maps. Although the teacher’s and student’s input pairs may have different baseline lengths, resulting in predicted disparity maps at different scales, the shared reference image captures the same absolute depth. According to Eq. (1), we have the equality below:

$$z = \frac{B^s \cdot f}{d^s} = \frac{B^t \cdot f}{d^t} \quad (4)$$

Student Network. We apply data augmentation only to input images of the student, including color jittering and random occlusion. By setting a more challenging optimization objective (Yang et al. 2024a), the student network is compelled to learn stronger and more robust feature representations to maintain accurate disparity predictions.

Teacher Network. The teacher network is initialized with the same weights as the student network. During training, the teacher’s gradients are truncated and its weights θ^t are updated by the student’s weights θ^s in each iteration. The update rule is $\theta^t \leftarrow m \cdot \theta^t + (1 - m) \cdot \theta^s$. The momentum parameter m follows the same cosine schedule as BYOL (Grill et al. 2020). In subsequent experiments, we show that the momentum teacher yields further performance gains compared to the fixed teacher. It also allows our framework to be trained from scratch without the well-pretrained teacher. During inference, disparity estimation is performed solely by the teacher network.

Occlusion-Aware Contrastive Loss

The student’s prediction d^s is supervised by the teacher’s prediction d^t with L_1 loss:

$$\mathcal{L}_c = \|d^s - r \cdot d^t\|_1 \quad (5)$$

where $r = B^s/B^t$ is the rescaling ratio that adjusts the teacher’s baseline length to match that of the student, derived from a transformation of Eq. (4).

Due to different target views available to the teacher and student, we partition each reference image into three regions: (1) non-occluded for both networks, (2) occluded for the teacher but not for the student, and (3) non-occluded for the teacher but occluded for the student. In region (2), the teacher often produces large errors, which can mislead the student. In region (3), the student cannot recover accurate disparities solely by matching priors, whereas the teacher’s predictions remain reliable. Moreover, we find that applying a uniform penalty across both occluded and non-occluded regions is insufficient to encourage the stereo network to learn effective occlusion completion, as shown in Fig. 4.

To this end, we construct an occlusion-aware attention map \mathcal{A} that excludes unreliable supervision in region (2) and emphasizes supervision in region (3). Since occluded regions naturally incur high photometric loss, we compute the teacher’s photometric loss \mathcal{L}_p^t , and apply a threshold τ to filter out occluded pixels for the teacher. We further employ the auto-masking strategy (Godard et al. 2019) to eliminate pixels with high uncertainty. Combining these two strategies yields a binary mask \mathcal{M}^t for the teacher. Similarly, we generate \mathcal{M}^s for the student. The occlusion-aware attention map \mathcal{A} is defined on a per-pixel basis as:

$$\mathcal{A} = \begin{cases} 0, & \text{if } \mathcal{M}^t = \text{False} \\ 1, & \text{if } \mathcal{M}^t = \text{True and } \mathcal{M}^s = \text{True} \\ 2, & \text{if } \mathcal{M}^t = \text{True and } \mathcal{M}^s = \text{False} \end{cases} \quad (6)$$

By applying this attention map on the contrastive loss \mathcal{L}_c , we provide accurate supervision to the student in both occluded and non-occluded regions, and further strengthen learning in regions that are teacher-friendly but student-challenging.

Deep networks trained with the contrastive loss may suffer from collapse to trivial solutions (Grill et al. 2020). For our framework, the teacher and student can take a shortcut by outputting a constant zero disparity, which causes \mathcal{L}_c to remain zero. To mitigate this problem, we further incorporate both the photometric loss \mathcal{L}_p^s and the smoothness loss \mathcal{L}_s^s in Eq. (2) and Eq. (3) as the auxiliary losses to facilitate the training of the student network.

The final loss is defined as follows:

$$\mathcal{L}_{total} = \mathcal{L}_c \odot \mathcal{A} + \lambda_p \mathcal{L}_p^s \odot \mathcal{M}^s + \lambda_s \mathcal{L}_s^s \quad (7)$$

where \odot is the element-wise multiplication. The parameter α in Eq. (2) is set to 0.85, and λ_s is set to $0.001\lambda_p$, following the configuration of Monodepth2 (Godard et al. 2019).

Synthetic Training Data

Existing stereo matching datasets provide only binocular images. To train stereo networks within our framework, we employ the CARLA simulator (Dosovitskiy et al. 2017) to

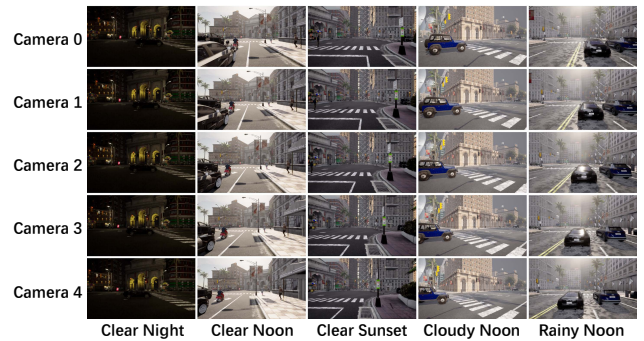


Figure 3: Examples of our synthetic dataset BaCon-20k for multi-baseline contrastive stereo matching.

synthesize multi-baseline stereo images. At each timestamp, we capture five horizontally displaced color images with a consistent baseline of 0.5 meters between the adjacent cameras. The images feature a focal length of 480 pixels and a resolution of 540×960 pixels. We collect 20,417 timestamps across seven towns under different lighting and weather conditions. Fig. 3 shows some representative examples.

Sampling Strategy of Triplet Input. In each iteration, we randomly select one reference image from the five images and sample two target images from the remaining four images, forming a triplet input. Notably, we do not restrict the target image to be physically on the right side of the reference. When the target lies to the left of the reference, we horizontally flip both images before feeding them into the network and flip the output back accordingly.

Experiments

Datasets and Evaluation Metrics

We train the stereo network on our synthetic dataset **BaCon-20k** and test on the following real-world datasets: KITTI 2015 (Menze and Geiger 2015), KITTI 2012 (Geiger, Lenz, and Urtasun 2012), Middlebury (Scharstein et al. 2014), ETH3D (Schops et al. 2017), and DrivingStereo (Yang et al. 2019). **KITTI 2015** and **KITTI 2012** are datasets of driving scenarios with hundreds of stereo images. **Middlebury** is a dataset of mixed indoor and outdoor scenarios, while **ETH3D** contains indoor scenario with grayscale stereo images. Both Middlebury and ETH3D have dozens of images. **DrivingStereo** provides specific weather conditions (sunny, cloudy, rainy, foggy). We evaluate the self-supervised fine-tuning performance on KITTI 2015 and KITTI 2012, the synthetic-to-real zero-shot generalization performance on KITTI 2015, KITTI 2012, Middlebury and ETH3D, and the robustness to diverse weather conditions on DrivingStereo.

We adopt **EPE** (end-point error) and **kpx** (percentage of outlier pixels with an absolute error greater than k pixels) as the evaluation metrics. For KITTI 2015, KITTI 2012, Middlebury, ETH3D, and DrivingStereo, the outlier thresholds k are set to 3, 3, 2, 1, and 3 respectively. All metrics are lower-better.

Method	KITTI 2015						KITTI 2012					
	NOC			ALL			NOC			ALL		
	D1-BG	D1-FG	D1-ALL	D1-BG	D1-FG	D1-ALL	EPE	>2px	>3px	EPE	>2px	>3px
SsSnet (arXiv 2017)	2.46	6.13	3.06	2.70	6.92	3.40	0.7	3.34	2.30	0.8	4.24	3.00
MC-CNN-WS (ICCV 2017)	3.06	9.42	4.11	3.78	10.93	4.97	0.8	4.76	3.02	1.0	6.57	4.45
OASM (ACCV 2018)	5.44	17.30	7.39	6.89	19.42	8.98	1.3	9.01	6.39	2.0	11.17	8.60
Flow2Stereo (CVPR 2020)	4.77	14.03	6.29	5.01	14.62	6.61	1.0	6.56	4.58	1.1	7.32	5.11
Reversing-PSM (ECCV 2020)	2.97	8.33	3.86	3.13	8.70	4.06	—	—	—	—	—	—
PVStereo (RA-L 2021)	2.09	5.73	2.69	2.29	6.50	2.99	0.7	4.55	1.98	0.8	5.25	2.47
PASMnet (T-PAMI 2022)	5.02	15.16	6.69	5.41	16.36	7.23	1.3	—	7.14	1.5	—	8.57
EMR-MSF (ICCV 2023)	8.30	14.16	9.27	8.61	15.15	9.70	—	—	—	—	—	—
UHP (RA-L 2024c)	4.65	12.37	5.93	5.00	13.70	6.45	1.2	9.08	6.05	1.3	10.37	7.09
DualNet (AAAI 2025)	2.28	4.66	2.67	2.46	5.25	2.92	0.6	—	2.06	0.6	—	2.59
BaCon-IGEV (Ours)	2.06	4.43	2.45	2.21	4.86	2.65	0.5	3.11	1.92	0.6	3.69	2.31
BaCon-IGEV[†] (Ours)	2.25	4.30	2.59	2.44	4.75	2.82	0.6	3.54	2.17	0.6	4.21	2.60

Table 1: **Quantitative results** on the KITTI 2015 and 2012 benchmarks. [†]BaCon-IGEV trained from scratch. KITTI 2015 and 2012 evaluate the performance in non-occluded (NOC) and all (ALL) regions. KITTI 2015 further reports the D1 metric (the proportion of outliers with an absolute error greater than 3 pixels and a relative error greater than 5%) in background (BG), foreground (FG), and all (ALL) regions. The **first**, **second**, and **third** are indicated by colors respectively.

Implementation Details

We employ IGEVStereo (Xu et al. 2023) as the backbones for the student and teacher networks. Following DualNet (Wang et al. 2025), we start from the official weights trained on SceneFlow (Mayer et al. 2016) and continue training for 200k iterations on our BaCon-20k on four NVIDIA 4090 GPUs. We use the Adam optimizer (Kingma and Ba 2017) and the one-cycle learning rate schedule (Smith 2018) with a maximum learning rate of $2e-4$. During training, the batch size is set to 16 and the input images are randomly cropped to a size of 256×512 pixels. λ_p is set to 10 and τ is set to 0.1 after hyper-parameter search.

Self-Supervised Fine-tuning Performance

In this section, we evaluate the self-supervised performance on KITTI 2015 (Menze and Geiger 2015) and 2012 (Geiger, Lenz, and Urtasun 2012) benchmarks.

Novel View Extrapolation. KITTI 2015 and 2012 only provide binocular image pair, which is not sufficient for our framework. Therefore, we extrapolate on both sides of the raw images with the generative model. Specifically, we use DEFOM-Stereo (Jiang et al. 2025) trained on KITTI to estimate the disparity maps for the raw left and right images. Next, we warp the left image further to the left using its estimated disparity, and similarly warp the right image further to the right. We then apply the Stable Diffusion v2 Inpainting model (SDv2I) (Rombach et al. 2022) to inpaint the occluded regions in warped images. In the experiments, we observe that the stereo network tends to oversmooth the edge disparity, causing bleeding artifacts (Xu et al. 2024) in the warped occlusion areas. These pixels should be marked for inpainting, but instead they degrade the generated appearance. To mitigate this problem, we dilate the inpainted mask before inpainting. Finally, as before, we sample image triplets from these four images to train the stereo network.

Fine-tuning Performance. We fine-tune on 14,184 triplets extended from 394 training pairs of KITTI 2015 and 2012 for one epoch, and submit the test set results to the

benchmarks for fair comparison with other self-supervised methods. As shown in Tab. 1, our BaCon-IGEV achieves state-of-the-art self-supervised performance across all metrics of the KITTI 2015 and 2012 benchmarks. It consistently outperforms previous self-supervised methods such as SsSnet (Zhong, Dai, and Li 2017) and PVStereo (Wang et al. 2021). Notably, SsSnet is trained on large-scale KITTI raw dataset (Geiger et al. 2013), while PVStereo leverages a pyramid voting strategy to generate pseudo-ground truth for supervision.

We also compare our method with DualNet (Wang et al. 2025). In DualNet, the student and teacher share the same occlusions, preventing the teacher from providing reliable guidance in occluded regions. Moreover, DualNet supervises the predicted probability distributions, which limits its compatibility with iterative methods. In contrast, our framework utilizes additional target cues to enable accurate supervision in both occluded and non-occluded regions, and is applicable to most stereo networks. Furthermore, the momentum teacher enables our framework to be trained from scratch while still achieving excellent self-supervised performance that is comparable to or even surpasses previous state-of-the-art methods. (see the last row of Tab. 1).

Zero-Shot Generalization Evaluation

The generalization capability of stereo networks is crucial for real-world deployment. We evaluate zero-shot generalization across real-world datasets with highly different scenarios. Unless otherwise specified, all compared methods are trained on the synthetic dataset SceneFlow (Mayer et al. 2016) and evaluated on the training sets of the real-world datasets (Menze and Geiger 2015; Geiger, Lenz, and Urtasun 2012; Scharstein et al. 2014; Schops et al. 2017).

As shown in Tab. 2, by applying the occlusion-attention contrastive loss to IGEVStereo (Xu et al. 2023), our method effectively reduces outliers in occluded regions by an average of 4.67%, while also greatly improving the prediction accuracy in the non-occluded regions. Our BaCon-IGEV

Method	KITTI 2015			KITTI 2012			Middlebury			ETH3D			#Params. (M)
	OCC	NOC	ALL	OCC	NOC	ALL	OCC	NOC	ALL	OCC	NOC	ALL	
PSMNet (CVPR 2018)	47.64	28.13	28.42	63.20	26.50	27.32	62.30	30.18	34.51	28.56	14.74	15.39	5.22
GwcNet (CVPR 2019)	29.07	12.17	12.53	45.65	11.91	12.67	47.13	20.41	24.11	21.37	10.49	11.09	6.91
CFNet (CVPR 2021)	16.42	5.87	6.10	30.25	4.58	5.15	44.55	16.33	20.22	11.89	5.57	5.87	23.05
RAFTStereo (3DV 2021)	12.70	5.34	5.53	28.35	4.29	4.84	28.00	9.06	11.96	6.02	2.85	3.04	11.12
ACVNet (CVPR 2022)	32.85	11.29	11.71	54.47	12.94	13.89	47.36	22.07	25.66	19.64	8.65	9.19	7.17
PCWNet (ECCV 2022)	14.95	5.53	5.74	30.22	4.07	4.67	37.99	12.17	15.86	11.67	5.28	5.54	35.94
IGEVStereo (CVPR 2023)	14.26	5.60	5.79	33.66	4.92	5.59	24.28	7.25	9.91	9.76	4.06	4.39	12.60
NerfStereo-RAFT [†] (CVPR 2023)	14.62	5.23	5.43	26.97	3.51	4.04	31.10	6.79	10.38	8.35	2.78	3.07	11.12
SelectiveIGEVStereo (CVPR 2024)	13.82	5.70	5.89	31.85	5.06	5.68	22.59	6.73	9.17	9.81	4.07	4.43	13.14
DEFOMStereo-L [‡] (CVPR 2025)	12.57	4.79	4.99	21.95	3.83	4.21	20.64	4.39	6.91	5.14	2.08	2.24	382.62
BaCon-IGEVStereo (Ours)	10.37	4.05	4.21	21.49	3.08	3.48	23.46	6.34	8.94	7.98	2.51	2.76	12.60

Table 2: **Zero-shot generalization across real-world datasets.** We report outlier metrics for occluded (OCC), non-occluded (NOC), and all (ALL) regions. All compared methods are re-evaluated using their officially released weights to ensure consistent benchmarking. [†]Method trained on real-world data with pseudo-ground truth. [‡]Vision foundation model-based method.



Figure 4: **Qualitative comparison** among IGEVStereo (Xu et al. 2023), Selective-IGEVStereo (Wang et al. 2024), and BaCon-IGEVStereo (Ours) in occluded regions of Middlebury (Scharstein et al. 2014).

ranks among the top three across all metrics, achieving performance comparable to DEFOMStereo-L (Jiang et al. 2025), but with $30\times$ fewer parameters. Furthermore, our method outperforms NerfStereo (Tosi et al. 2023) in both occluded and non-occluded regions. Although NerfStereo leverages photometric loss from a non-occluded third view during back-propagation, this design primarily enhances matching performance rather than explicitly encouraging occlusion completion. These results highlight the effectiveness of our BaCon-Stereo framework in guiding the stereo network to learn both accurate matching in non-occluded regions and effective completion in occluded regions.

As shown in Fig. 4, both IGEVStereo (Xu et al. 2023) and Selective-IGEVStereo (Wang et al. 2024) apply the uniform supervision strength to occluded and non-occluded regions, often resulting in inaccurate predictions in occluded regions. In contrast, our BaCon-IGEVStereo significantly improves this issue, benefiting from the contrastive loss guided by the occlusion-aware attention map.

Robustness across Different Weathers

For stereo vision-based systems operating outdoors, the robustness under challenging weather conditions is essential. Tab. 3 shows that our method achieves superior cross-weather robustness on DrivingStereo (Yang et al. 2019). Compared to IGEVStereo, we reduce the proportion of outliers in sunny, cloudy, rainy, and foggy conditions to at least half of the original. Notably, under rainy conditions, where all competing methods produce over 10% outliers and thus pose serious risks to stereo vision-based systems, our method maintains robust accuracy with only 5.07% outliers.

Method	Sunny	Cloudy	Rainy	Foggy
PSMNet (2018)	40.14	43.95	56.19	69.69
GwcNet (2019)	17.12	25.56	28.19	29.23
CFNet (2021)	4.70	5.30	12.48	5.54
RAFTStereo (2021)	4.23	4.19	12.77	3.09
ACVNet (2022)	19.64	29.87	41.31	38.05
PCWNet (2022)	3.58	3.67	10.52	5.20
IGEVStereo (2023)	4.59	5.15	15.47	4.49
NerfStereo [†] (2023)	2.88	2.91	10.20	3.93
Selective-IGEVStereo (2024)	5.05	5.24	13.51	4.10
DEFOMStereo [‡] (2025)	3.61	3.75	13.53	2.88
BaCon-IGEVStereo (Ours)	2.15	1.87	5.07	1.64

Table 3: **Robustness across different weathers** on DrivingStereo (Yang et al. 2019). Outliers ($>3px$) are reported. [†]Method trained on real-world data with pseudo-ground truth. [‡]Vision foundation model-based method.

These gains are primarily attributed to our overall framework, which combines data augmentation for the student with the momentum update strategy for the teacher to facilitate effective learning. The student must learn strong feature representations, along with robust matching and completion capabilities, to handle the open world. Therefore, even without foggy samples during training, our method still exhibits strong performance under foggy conditions.

Fig. 5 presents qualitative results on rainy and foggy conditions. Specifically, both IGEVStereo and Selective-IGEVStereo fail on water-logged road surfaces, whereas our method still predicts accurate disparities.

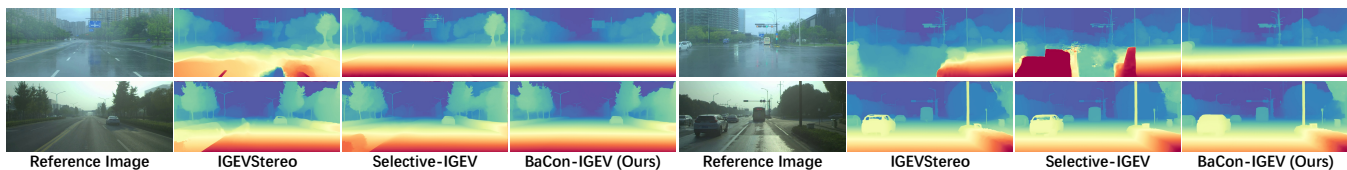


Figure 5: **Qualitative comparison** among IGEVStereo (Xu et al. 2023), Selective-IGEV (Wang et al. 2024), and BaCon-IGEV (Ours) on the rainy (top row) and foggy (bottom row) subsets of DrivingStereo (Yang et al. 2019).

	\mathcal{L}_c	\mathcal{L}_p	\mathcal{L}_s	OCC	NOC	ALL
(A)		✓	✓	97.44	5.51	7.14
(B)	✓			11.22	5.23	5.38
(C)	✓	✓		10.62	4.49	4.64
(D)	✓		✓	11.23	5.14	5.29
(E)	✓	✓	✓	10.37	4.05	4.21
(E)*	✓	✓	✓	10.87	4.98	5.12

Table 4: **Ablation study** of loss terms in Eq. (7). *EMA is not used to update the teacher network.

Threshold	Auto-Mask	Occ-Aware	OCC	NOC	ALL
			13.67	4.93	5.13
✓			13.49	4.76	4.96
	✓		13.27	4.43	4.64
✓	✓		12.39	4.06	4.25
✓	✓	✓	10.37	4.05	4.21

Table 5: **Ablation study** of the valid masks and occlusion-aware attention map.

Ablation Study

We validate the effectiveness of our method through comprehensive ablations. All variants are trained on our BaCon-20k dataset and reported outliers ($>3\text{px}$) for occluded (OCC), non-occluded (NOC), and all (ALL) regions on the KITTI 2015 training set (Menze and Geiger 2015).

Loss Terms. As shown in Tab. 4, conventional self-supervised losses (A) fail to provide effective supervision for occluded regions, resulting in almost completely erroneous predictions. This limitation stems from the inherent inability of photometric supervision to provide reliable learning signals in occluded regions, where no true correspondence exists between stereo images. Without proper handling, models tend to overfit incorrect photometric cues, leading to erroneous disparity predictions in these challenging regions. Conversely, our contrastive loss (B) addresses this issue by exploiting multi-baseline geometric consistency, achieving simultaneous performance gains in both occluded and non-occluded regions. We further investigate the combinations of these loss functions (C)-(E). Quantitative results confirm that the integrated loss (E) provides the optimal results.

Momentum Teacher. In Tab. 4, we further prove the benefit of the momentum teacher. Compared to the fixed teacher (E)*, the momentum teacher (E) offers more stable and generalizable supervision, leading to consistent improvements in all regions.

Occlusion-Aware Attention Map. We ablate the two

Method	OCC	NOC	ALL
GwcNet (CVPR 2019)	29.07	12.17	12.53
BaCon-Gwc (Ours)	12.70	4.46	4.65
CFNet (CVPR 2021)	16.42	5.87	6.10
BaCon-CF (Ours)	11.88	4.26	4.44
RAFTStereo (3DV 2021)	12.70	5.34	5.53
BaCon-RAFT (Ours)	11.73	3.92	4.09

Table 6: **Generality** of our framework. We additionally test the 3D convolution-based backbones GwcNet (Guo et al. 2019) and CFNet (Shen, Dai, and Rao 2021), and the iteration-based backbone RAFTStereo (Lipson, Teed, and Deng 2021).

strategies used to generate the binary mask. As shown in Tab. 5, the auto-masking strategy (Godard et al. 2019) effectively improves the performance by removing pixels with high uncertainty (*i.e.*, weakly-textured regions and areas at infinity). Building on this, filtering out occluded pixels that inherently exhibit significant photometric loss further enhances the quality of the mask, reducing noise in supervision signals and achieving superior disparity prediction. By imposing stronger supervision on occluded regions, the stereo network achieves significant improvements in these challenging regions, demonstrating the effectiveness of our occlusion-aware mechanism.

Generality. Our contrastive loss directly supervises the predicted disparity map, making our framework applicable to various types of stereo backbones. We evaluate its generality on both the 3D convolution-based backbones (Guo et al. 2019; Shen, Dai, and Rao 2021) and the iteration-based backbone (Lipson, Teed, and Deng 2021). As shown in Tab. 6, our method consistently improves performance over all three baselines. While RAFTStereo already performs well in occluded regions, our method further enhances its completion capability from 12.70% to 11.73%.

Conclusion

In this paper, we propose BaCon-Stereo, a self-supervised teacher-student framework trained via multi-baseline contrastive learning. By exploiting different non-occluded regions between the teacher and student, we provide reliable supervision for the student across both occluded and non-occluded areas. In addition, we introduce an occlusion-aware attention map to guide the student in learning accurate disparity completion for occluded regions. To validate the effectiveness of our method, we construct BaCon-20k, a multi-baseline stereo dataset covering diverse lighting and

weather conditions. Experimental results demonstrate that our method matches or surpasses existing methods in generalization across varied scenarios and in robustness under different weathers. We also outperform previous self-supervised methods on KITTI 2015 and 2012 benchmarks.

References

- Aleotti, F.; Tosi, F.; Zhang, L.; Poggi, M.; and Mattocchia, S. 2020. Reversing the cycle: self-supervised deep stereo through enhanced monocular distillation. In *European Conference on Computer Vision*, 614–632. Springer.
- Arpit, D.; Jastrzebski, S.; Ballas, N.; Krueger, D.; Bengio, E.; Kanwal, M. S.; Maharaj, T.; Fischer, A.; Courville, A.; Bengio, Y.; et al. 2017. A closer look at memorization in deep networks. In *International conference on machine learning*, 233–242. PMLR.
- Bai, T.; Xiang, Z.; Zhao, X.; Xu, P.; Pu, T.; and Fu, J. 2025. LiDAR semantic segmentation with local consistency constrained KPConv LSTM. *Neurocomputing*, 626: 129542.
- Caron, M.; Touvron, H.; Misra, I.; Jégou, H.; Mairal, J.; Bojanowski, P.; and Joulin, A. 2021. Emerging properties in self-supervised vision transformers. In *Proceedings of the IEEE/CVF international conference on computer vision*, 9650–9660.
- Chang, J.-R.; and Chen, Y.-S. 2018. Pyramid stereo matching network. In *Proceedings of the IEEE conference on computer vision and pattern recognition*, 5410–5418.
- Chen, S.; Xiang, Z.; Xu, P.; and Zhao, X. 2022. A normalized disparity loss for stereo matching networks. *IEEE Robotics and Automation Letters*, 8(1): 33–40.
- Dosovitskiy, A.; Ros, G.; Codevilla, F.; Lopez, A.; and Koltun, V. 2017. CARLA: An open urban driving simulator. In *Conference on robot learning*, 1–16. PMLR.
- Geiger, A.; Lenz, P.; Stiller, C.; and Urtasun, R. 2013. Vision meets Robotics: The KITTI Dataset. *International Journal of Robotics Research (IJRR)*.
- Geiger, A.; Lenz, P.; and Urtasun, R. 2012. Are we ready for autonomous driving? the kitti vision benchmark suite. In *2012 IEEE conference on computer vision and pattern recognition*, 3354–3361. IEEE.
- Godard, C.; Mac Aodha, O.; Firman, M.; and Brostow, G. J. 2019. Digging into self-supervised monocular depth estimation. In *Proceedings of the IEEE/CVF international conference on computer vision*, 3828–3838.
- Grill, J.-B.; Strub, F.; Altché, F.; Tallec, C.; Richemond, P.; Buchatskaya, E.; Doersch, C.; Avila Pires, B.; Guo, Z.; Gheshlaghi Azar, M.; et al. 2020. Bootstrap your own latent—a new approach to self-supervised learning. *Advances in neural information processing systems*, 33: 21271–21284.
- Guo, X.; Yang, K.; Yang, W.; Wang, X.; and Li, H. 2019. Group-wise correlation stereo network. In *Proceedings of the IEEE/CVF Conference on Computer Vision and Pattern Recognition*, 3273–3282.
- He, K.; Fan, H.; Wu, Y.; Xie, S.; and Girshick, R. 2020. Momentum contrast for unsupervised visual representation learning. In *Proceedings of the IEEE/CVF conference on computer vision and pattern recognition*, 9729–9738.
- Jiang, H.; Lou, Z.; Ding, L.; Xu, R.; Tan, M.; Jiang, W.; and Huang, R. 2025. DEFOM-Stereo: Depth Foundation Model Based Stereo Matching. *arXiv preprint arXiv:2501.09466*.
- Jiang, Z.; and Okutomi, M. 2023. EMR-MSF: Self-Supervised Recurrent Monocular Scene Flow Exploiting Ego-Motion Rigidity. In *Proceedings of the IEEE/CVF International Conference on Computer Vision*, 69–78.
- Kingma, D. P.; and Ba, J. 2017. Adam: A Method for Stochastic Optimization. arXiv:1412.6980.
- Li, A.; and Yuan, Z. 2018. Occlusion aware stereo matching via cooperative unsupervised learning. In *Asian Conference on Computer Vision*, 197–213. Springer.
- Li, J.; Wang, P.; Xiong, P.; Cai, T.; Yan, Z.; Yang, L.; Liu, J.; Fan, H.; and Liu, S. 2022. Practical stereo matching via cascaded recurrent network with adaptive correlation. In *Proceedings of the IEEE/CVF Conference on Computer Vision and Pattern Recognition*, 16263–16272.
- Lipson, L.; Teed, Z.; and Deng, J. 2021. Raft-stereo: Multilevel recurrent field transforms for stereo matching. In *2021 International Conference on 3D Vision (3DV)*, 218–227. IEEE.
- Liu, P.; King, I.; Lyu, M. R.; and Xu, J. 2020. Flow2stereo: Effective self-supervised learning of optical flow and stereo matching. In *Proceedings of the IEEE/CVF conference on computer vision and pattern recognition*, 6648–6657.
- Mayer, N.; Ilg, E.; Hausser, P.; Fischer, P.; Cremers, D.; Dosovitskiy, A.; and Brox, T. 2016. A large dataset to train convolutional networks for disparity, optical flow, and scene flow estimation. In *Proceedings of the IEEE conference on computer vision and pattern recognition*, 4040–4048.
- Menze, M.; and Geiger, A. 2015. Object scene flow for autonomous vehicles. In *Proceedings of the IEEE conference on computer vision and pattern recognition*, 3061–3070.
- Rombach, R.; Blattmann, A.; Lorenz, D.; Esser, P.; and Ommer, B. 2022. High-resolution image synthesis with latent diffusion models. In *Proceedings of the IEEE/CVF conference on computer vision and pattern recognition*, 10684–10695.
- Scharstein, D.; Hirschmüller, H.; Kitajima, Y.; Krathwohl, G.; Nešić, N.; Wang, X.; and Westling, P. 2014. High-resolution stereo datasets with subpixel-accurate ground truth. In *German conference on pattern recognition*, 31–42. Springer.
- Scharstein, D.; and Szeliski, R. 2002. A taxonomy and evaluation of dense two-frame stereo correspondence algorithms. *International journal of computer vision*, 47(1): 7–42.
- Schops, T.; Schonberger, J. L.; Galliani, S.; Sattler, T.; Schindler, K.; Pollefeys, M.; and Geiger, A. 2017. A multi-view stereo benchmark with high-resolution images and multi-camera videos. In *Proceedings of the IEEE Conference on Computer Vision and Pattern Recognition*, 3260–3269.
- Shen, Z.; Dai, Y.; and Rao, Z. 2021. Cfnet: Cascade and fused cost volume for robust stereo matching. In *Proceedings of the IEEE/CVF Conference on Computer Vision and Pattern Recognition*, 13906–13915.

- Shen, Z.; Dai, Y.; et al. 2022. PCW-Net: Pyramid Combination and Warping Cost Volume for Stereo Matching. In *ECCV*.
- Smith, L. N. 2018. A disciplined approach to neural network hyper-parameters: Part 1 – learning rate, batch size, momentum, and weight decay. [arXiv:1803.09820](https://arxiv.org/abs/1803.09820).
- Tosi, F.; Tonioni, A.; De Gregorio, D.; and Poggi, M. 2023. Nerf-supervised deep stereo. In *Proceedings of the IEEE/CVF conference on computer vision and pattern recognition*, 855–866.
- Tulyakov, S.; Ivanov, A.; and Fleuret, F. 2017. Weakly supervised learning of deep metrics for stereo reconstruction. In *Proceedings of the IEEE International Conference on Computer Vision*, 1339–1348.
- Wang, H.; Fan, R.; Cai, P.; and Liu, M. 2021. PVStereo: Pyramid voting module for end-to-end self-supervised stereo matching. *IEEE Robotics and Automation Letters*, 6(3): 4353–4360.
- Wang, L.; Guo, Y.; Wang, Y.; Liang, Z.; Lin, Z.; Yang, J.; and An, W. 2022. Parallax Attention for Unsupervised Stereo Correspondence Learning. *IEEE Transactions on Pattern Analysis and Machine Intelligence*, 44(4): 2108–2125.
- Wang, X.; Xu, G.; Jia, H.; and Yang, X. 2024. Selective-stereo: Adaptive frequency information selection for stereo matching. In *Proceedings of the IEEE/CVF Conference on Computer Vision and Pattern Recognition*, 19701–19710.
- Wang, Y.; Zheng, J.; Zhang, C.; Zhang, Z.; Li, K.; Zhang, Y.; and Hu, J. 2025. DualNet: Robust Self-Supervised Stereo Matching with Pseudo-Label Supervision. In *Proceedings of the AAAI Conference on Artificial Intelligence*, volume 39, 8178–8186.
- Wang, Z.; Bovik, A. C.; Sheikh, H. R.; and Simoncelli, E. P. 2004. Image quality assessment: from error visibility to structural similarity. *IEEE transactions on image processing*, 13(4): 600–612.
- Wu, Z.; Xiong, Y.; Yu, S. X.; and Lin, D. 2018. Unsupervised feature learning via non-parametric instance discrimination. In *Proceedings of the IEEE conference on computer vision and pattern recognition*, 3733–3742.
- Xu, G.; Cheng, J.; Guo, P.; and Yang, X. 2022. Attention Concatenation Volume for Accurate and Efficient Stereo Matching. In *Proceedings of the IEEE/CVF Conference on Computer Vision and Pattern Recognition*, 12981–12990.
- Xu, G.; Wang, X.; Ding, X.; and Yang, X. 2023. Iterative Geometry Encoding Volume for Stereo Matching. In *Proceedings of the IEEE/CVF Conference on Computer Vision and Pattern Recognition*, 21919–21928.
- Xu, P.; Xiang, Z.; Fu, J.; Pu, T.; Zhong, H.; and Liu, E. 2025a. MIDAS: Modeling Ground-Truth Distributions with Dark Knowledge for Domain Generalized Stereo Matching. [arXiv preprint arXiv:2503.04376](https://arxiv.org/abs/2503.04376).
- Xu, P.; Xiang, Z.; Qiao, C.; Fu, J.; and Pu, T. 2024. Adaptive Multi-Modal Cross-Entropy Loss for Stereo Matching. In *Proceedings of the IEEE/CVF Conference on Computer Vision and Pattern Recognition*, 5135–5144.
- Xu, R.; Xiang, Z.; Zhang, C.; Zhong, H.; Zhao, X.; Dang, R.; Xu, P.; Pu, T.; and Liu, E. 2025b. SCKD: Semi-supervised cross-modality knowledge distillation for 4d radar object detection. In *Proceedings of the AAAI Conference on Artificial Intelligence*, volume 39, 8933–8941.
- Yang, G.; Song, X.; Huang, C.; Deng, Z.; Shi, J.; and Zhou, B. 2019. Drivingstereo: A large-scale dataset for stereo matching in autonomous driving scenarios. In *Proceedings of the IEEE/CVF conference on computer vision and pattern recognition*, 899–908.
- Yang, L.; Kang, B.; Huang, Z.; Xu, X.; Feng, J.; and Zhao, H. 2024a. Depth anything: Unleashing the power of large-scale unlabeled data. In *Proceedings of the IEEE/CVF Conference on Computer Vision and Pattern Recognition*, 10371–10381.
- Yang, L.; Kang, B.; Huang, Z.; Zhao, Z.; Xu, X.; Feng, J.; and Zhao, H. 2024b. Depth anything v2. *Advances in Neural Information Processing Systems*, 37: 21875–21911.
- Yang, R.; Li, X.; Cong, R.; and Du, J. 2024c. Unsupervised hierarchical iterative tile refinement network with 3D planar segmentation loss. *IEEE Robotics and Automation Letters*, 9(3): 2678–2685.
- Žbontar, J.; and LeCun, Y. 2016. Stereo matching by training a convolutional neural network to compare image patches. *Journal of Machine Learning Research*, 17(65): 1–32.
- Zhong, H.; Xiang, Z.; Xu, R.; Fu, J.; Xu, P.; Wang, S.; Yang, Z.; Pu, T.; and Liu, E. 2025. CVFusion: Cross-View Fusion of 4D Radar and Camera for 3D Object Detection. [arXiv preprint arXiv:2507.04587](https://arxiv.org/abs/2507.04587).
- Zhong, Y.; Dai, Y.; and Li, H. 2017. Self-supervised learning for stereo matching with self-improving ability. [arXiv preprint arXiv:1709.00930](https://arxiv.org/abs/1709.00930).